Journal of Power Sources 196 (2011) 5731–5736

Contents lists available at ScienceDirect

Journal of Power Sources

journal homepage: www.elsevier.com/locate/jpowsour

Crystalline CoB: Solid state reaction synthesis and electrochemical properties

Yaping Wang [a], Li Li [a], Yijing Wang [a,*], Dawei Song [b], Guang Liu [a], Yan Han [a], Lifang Jiao [a], Huatang Yuan [a]

[a] Institute of New Energy Material Chemistry, Key Laboratory of Advanced Energy Materials Chemistry (MOE), Nankai University, Tianjin 300071, PR China
[b] School of Chemistry and Chemical Engineering, Henan University of Technology, Zhengzhou 450001, PR China

ARTICLE INFO

Article history:
Received 15 September 2010
Received in revised form 22 January 2011
Accepted 31 January 2011
Available online 23 February 2011

Keywords:
Nickel-based secondary battery
Cobalt boride
Solid state reaction
Electrochemistry
Reaction mechanism

ABSTRACT

Using a facile and effective method based on the solid phase reaction between $Co(OH)_2$ and KBH_4, we successfully synthesize orthorhombic CoB. It is shown that this CoB obtained is of high purity and thermal stability. A possible formation process for orthorhombic CoB is discussed in detail. In addition, crystalline CoB shows excellent electrochemical reversibility and considerable high charge–discharge capacities when it is used as the anode material for nickel-based secondary batteries. The reversible discharge capacities of the CoB electrode are found to be about 380 mAh g^{-1} at a discharge current of 25 mA g^{-1} and 360 mAh g^{-1} at 100 mA g^{-1}. Moreover, electrochemical reaction mechanism of CoB is investigated in detail.

1. Introduction

There has been much progress in preparing transition metal borides (M–B, M = Fe, Co, Ni), stimulated by the interest in ferrofluids, powder metallurgy, magnetic applications, composite materials, and catalysis applications [1–12]. In recent years, Co–B, as one of the transition metal borides, has been frequently reported as an anode material for nickel-based secondary batteries [13–17], largely due to its high discharge capacity and excellent cycling performance. However, to date, almost all of them have focused on the electrochemical properties of Co–B with amorphous structure, few studies have been reported on the crystalline structures [18]. The reason is that the amorphous structure of Co–B with nano sizes could be easily obtained by chemical reduction of cobalt salt with $NaBH_4$/KBH_4 in an aqueous or ethanolic solution [19]. Unfortunately, the composition of this Co–B is usually unmanageable and the structure is unstable, and thus the electrochemical mechanism is contentious. Using a crystalline structure is a feasible route to investigate its reaction mechanism.

Typically, crystalline transition metal borides are prepared by arc melting of the pure metal and boron [20–22]. However, because of the high melting points of metal and boron, it requires extremely high reaction temperature (>2000 °C). Moreover, the alloys obtained are bulky, and impurity phases such as pure metals, metal oxides, and B_2O_3 are always simultaneously produced. Therefore, it is necessary to develop an alternative method for preparing high-purity crystalline transition metal borides with nano sizes at a lower temperature.

According to the bulk phase diagram, the Co–B system consists of three intermediate compounds, Co_3B, Co_2B and CoB. A key question is what phase of cobalt boride will be produced if chemical reactions are carried out with or without stoichiometric control. This paper reports a new way to prepare highly crystalline cobalt boride with phase control by the solid phase reaction of $Co(OH)_2$ and KBH_4. In this particular method, KBH_4 is used as not only a boron precursor but also a reducing agent. High purity and thermal stability of orthorhombic CoB can be successfully obtained and electrochemically used as the anode material for nickel-based secondary batteries. The structural and electrochemical characteristics of the crystalline CoB are discussed. Moreover, the electrochemical reaction mechanism of CoB is investigated in detail.

2. Experimental

In a typical procedure, $Co(OH)_2$ (0.005 mol, prepared by precipitation method) was homogeneously mixed with KBH_4 (0.01 mol, 98.0%) in a carnelian mortar. The mixture was pressed into a small pellet of 10 mm in diameter under 20 MPa pressure. Then, the pellet was heated at 600 °C for 12 h and cooled to room temperature under a flow of Ar (99.999%). The black solid obtained was washed thoroughly with distilled water and absolute ethyl alcohol to remove the by-products. After that, the wet products were dried in vacuum at 80 °C for 12 h.

Crystalline structure of CoB sample was determined by X-ray powder diffraction (XRD, Rigaku D/Max-2500 with Cu Kα radiation), and selective area electronic diffraction (SAED, JEOL

* Corresponding author. Tel.: +86 22 23503639; fax: +86 22 23503639.
E-mail address: wangyj@nankai.edu.cn (Y. Wang).

0378-7753/$ – see front matter © 2011 Elsevier B.V. All rights reserved.
doi:10.1016/j.jpowsour.2011.01.104

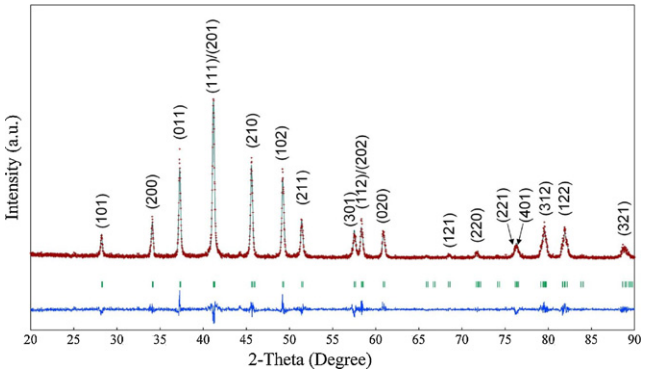

Fig. 1. X-ray diffraction profile of CoB sample: observed (red points), calculated (green line), and difference (bottom blue line). Vertical bars below the patterns show the positions of all possible reflection peaks. The *h k l* labels are placed according to the reflection position. (For interpretation of the references to color in this figure legend, the reader is referred to the web version of this article.)

JEM-2100). XRD patterns were refined by RIETAN-2000 [23]. Surface morphology was evaluated by transmission electron microscopy (TEM, JEOL JEM-2100). Electronic states were investigated by X-ray photoelectron spectroscopy (XPS, Kratos Axis Ultra DLD spectrometer with Al Kα radiation), during which CoB samples were etched for 10 min to avoid surface oxidation. All of the binding energy values were calibrated using C 1s = 284.6 eV as a reference. Thermal stability of CoB sample was performed by simultaneous thermogravimetry–differential scanning calorimetry (TG–DSC, NETZSCH STA-409PC) under N_2 (99.999%) atmosphere at a heating rate of 5 °C min^{-1}.

Quantitative temperature hydrogen absorption curve was determined by volumetric methods with a home-made Sieverts-type apparatus. For each experiment, 200 mg of CoB powder sample was loaded into a stainless-steel tube reactor, which was connected to a Sieverts-type apparatus. Then, the sample was gradually heated to 300 °C at an average ramp of 1 °C min^{-1} and kept for 12 h. Temperatures and pressures of the sample and gas reservoirs were automatically monitored and recorded.

For electrochemical measurements, the CoB electrodes were constructed through mixing the products with carbonyl nickel powders in a weight ratio of 1:3. The powder mixtures were pressed under 30 MPa pressure into a small pellet of 10 mm in diameter. Then, the electrodes were conducted in a three compartment cell using a LAND battery test instrument (CT2001A). NiOOH/$Ni(OH)_2$ and Hg/HgO were used as the counter electrode and the reference electrode, respectively. The electrolyte was a 6 M KOH aqueous solution. Charge–discharge cycle tests were carried out at the current of 25 and 100 mA g^{-1}. The cut-off voltage for discharge test was −0.5 V (vs. Hg/HgO). The testing interval between charge and discharge was 5 min. Zahner IM6e electrochemical workstation was used for cyclic voltammetry (scan rate: 0.1, 0.2, 0.5 and 1 mV s^{-1}, potential interval: −1.2 V to −0.4 V, vs. Hg/HgO). All the experiments were conducted at room temperature.

3. Results and discussion

3.1. Material characterization

Fig. 1 shows the representative Rietveld refinement of XRD patterns of the sample. It reveals that the sample obtained is homogeneous and crystalline. The diffraction peaks well match that of orthorhombic structure CoB (space group *Pnma*, JCPDS no. 65-2596). No peak from other phase such as crystalline Co, Co_2B, or Co_3B has been detected in the samples, revealing that the CoB obtained is of high purity. The lattice parameters a = 5.255 Å, b = 3.043 Å, c = 3.955 Å from the diffraction pattern are in good agreement with literature values for orthorhombic CoB. Furthermore, the refined patterns fit the observed data points very well, further confirms the pure phase of CoB.

Fig. 2a and b shows low- and high-magnification TEM images of orthorhombic CoB. They mainly present in spherical shape with diameters of several tens to several hundreds of nanometers which is similar to the reported amorphous Co–B. The HRTEM image in Fig. 2c clearly reveals a lattice spacing of 0.220 nm corresponding to the (1 1 1)/(2 0 1) plane of orthorhombic CoB. The SAED image (Fig. 2d) displays many diffraction spots, suggesting a crystalline structure of CoB. To study the electronic interaction between the atoms in the compound, XPS spectra of CoB are acquired and reported in Fig. 2e and f. A peak with binding energy (BE) of 777.8 eV is observed in the $Co_{2p3/2}$ level, and accordingly, a peak with BE of 188.0 eV occurs in the B_{1s} level, indicating that Co and B exist in the state of CoB. This also validates the high-purity of CoB obtained.

Transition metal borides with amorphous structures are always thermal unstable, which greatly restricts their applications in high temperature conditions. Therefore, we also investigate the thermal stability of as-prepared CoB. TG and DSC curves of CoB are showed in Fig. 3. There is no noticeable endothermic/exothermic peak and weight loss from room temperature to 400 °C, indicating a high thermal stability of CoB obtained.

3.2. Investigation of the formation process

In order to understand the solid state reaction between $Co(OH)_2$ and KBH_4, a series of experiments are carried out. Fig. 4 shows the XRD patterns of the products before and after rinsing. As compared to the final products, the sample obtained without rinsing is composed of CoB and KBO_2. The molar ratio of CoB/KBO_2 calculated by RIETAN-2000 is about 55%/45% [23]. Compared to the ratio of raw materials, about half of the K and some H are lost. TG profile of $Co(OH)_2$ and KBH_4 mixture ($Co(OH)_2/KBH_4$ = 1/2) is illustrated in Fig. 5. There are two noticeable weight losses occurred. The weight loss around 200 °C is obviously due to the decomposition of $Co(OH)_2$. Ostroff and Sanderson [24] studied the behavior of KBH_4 heated in nitrogen, and found that metal K, B and H_2 were generated at 584 °C and the metal K was lost by volatilization. Thus, the weight loss from 480 °C to 560 °C may be attributed to the metal K and H_2. This can be confirmed by the mass loss of 20.58% and the existence of K in the exhaust (determined by flame reaction). In this procedure, the decomposition temperature of KBH_4 is lower than reported, showing that $Co(OH)_2$ (may be CoO or CoB) has a catalytic activity for the thermal decomposition of KBH_4.

Based on these experimental facts and materials and charge balances, the solid reaction between $Co(OH)_2$ and KBH_4 for the production of CoB could be suggested as follows:

$$2Co(OH)_2 + 3KBH_4 = 2CoB + KBO_2 + 2K + 6H_2 + 2H_2O \quad (1)$$

According to this equation, the minimum ratio of $Co(OH)_2/KBH_4$ should be 1.5 for converting all $Co(OH)_2$ to CoB. Therefore, KBH_4 is superfluous in this work, which would react with the H_2O contained in $Co(OH)_2$ to form KBO_2. Furthermore, it is concluded that using cobalt oxides (Co_3O_4, Co_2O_3 and CoO) instead of $Co(OH)_2$ as cobalt precursors is a possible way to obtain orthorhombic CoB.

3.3. Electrochemical performance

Fig. 6a shows the typical cyclic voltammogram (CV) curves of CoB electrode in 6 M KOH aqueous solution. For the CV curve with the scanning rate of 1 mV s^{-1}, a remarkable reduction peak appears at −1.07 V, and correspondingly, a strong oxidation peak arises at −0.61 V, respectively, suggesting a reversible electrochemical

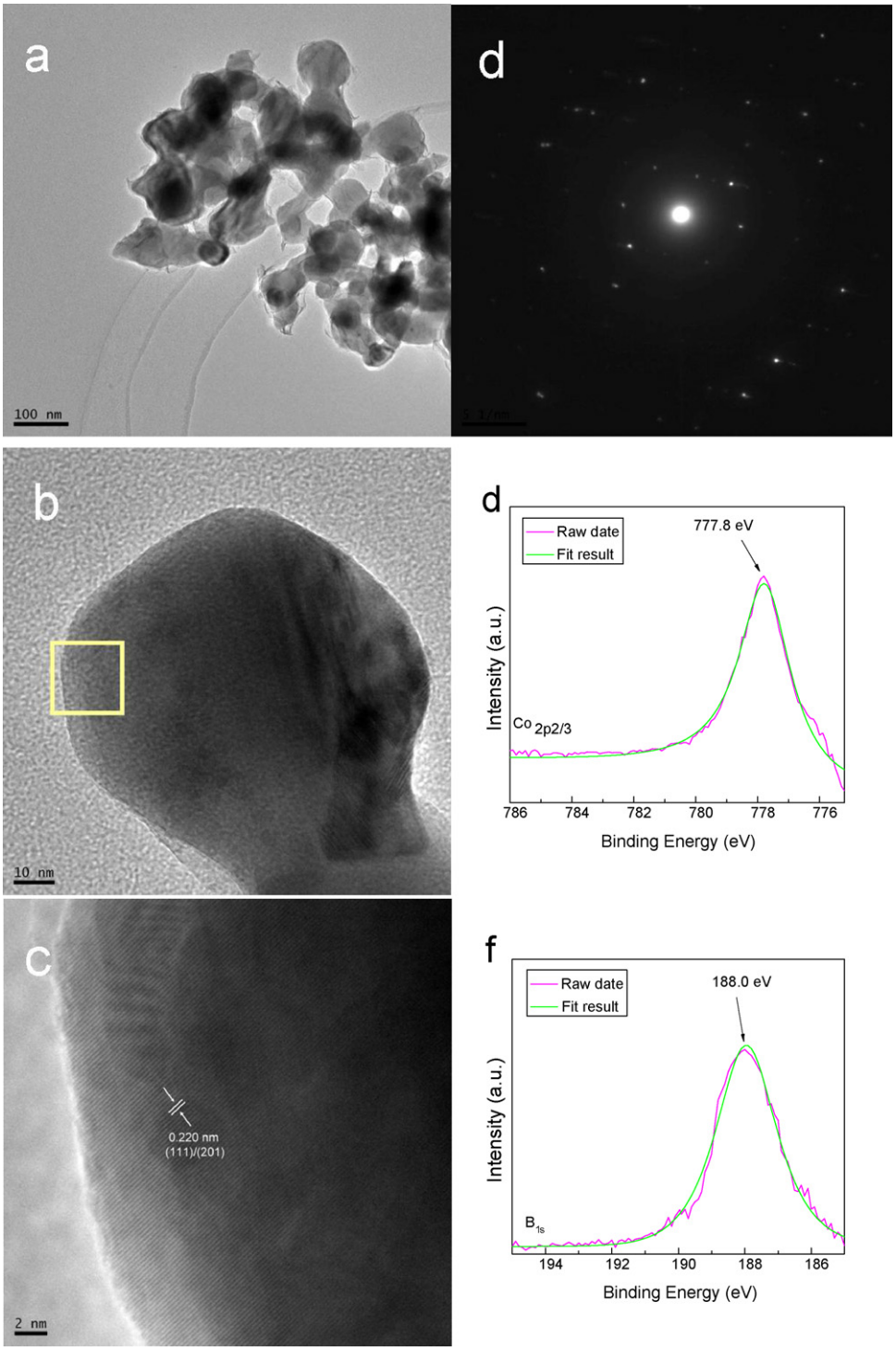

Fig. 2. (a) TEM and (b and c) HRTEM images of as-prepared orthorhombic CoB. (d) The SAED image. XPS spectra of (e) $Co_{2p2/3}$ and (f) B_{1s} for CoB obtained.

reaction occurring on the CoB electrode. When the scanning rate decreases, the potential of the oxidation peak decreases, while the reduction peak increases, indicating that the faster the scanning rate is, the more serious the polarization will be. Fig. 6b shows the liner relationship between the peak current and the square root of the scanning rate $\nu^{1/2}$. It implies that the electrochemical reactions of CoB electrode in 6 M KOH solution are diffusion-controlled reactions.

Fig. 6c shows the cycling performances of CoB electrodes at different discharge rates. At the initial cycle, the CoB electrodes show exceptionally high irreversible discharge capacities (728 mAh g^{-1} at 25 mA g^{-1} and 393 mAh g^{-1} at 100 mA g^{-1}), which is similar to amorphous Co–B electrode reported [14]. When the discharge current is 25 mA g^{-1}, the reversible capacity is stabilized at about 380 mAh g^{-1} from the fifth cycle. Even after 50 cycles, the reversible capacity is still kept up at more than 360 mAh g^{-1}, showing quite good capacity retention. The reversible capacity of the CoB electrode at the high discharge current of 100 mA g^{-1} is about 360 mAh g^{-1}, which occurs at the tenth cycle. After 50 cycles, it remains more than 325 mAh g^{-1}, showing excellent rate capability.

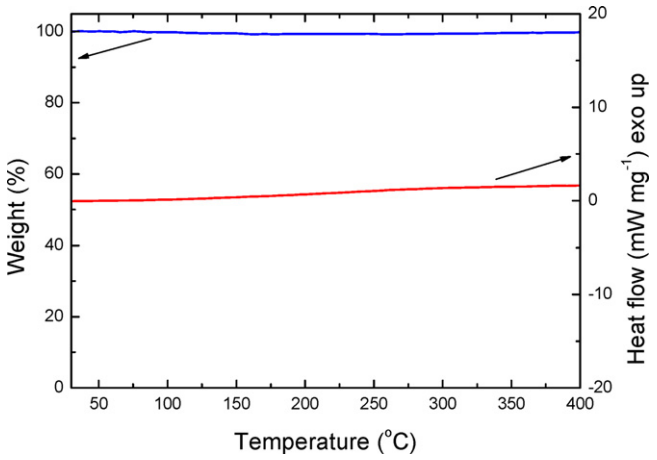

Fig. 3. TG and DSC curves of orthorhombic CoB.

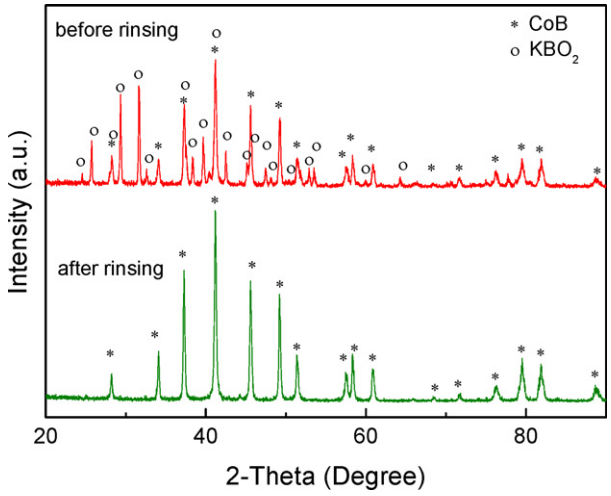

Fig. 4. XRD patterns of the products before and after rinsing.

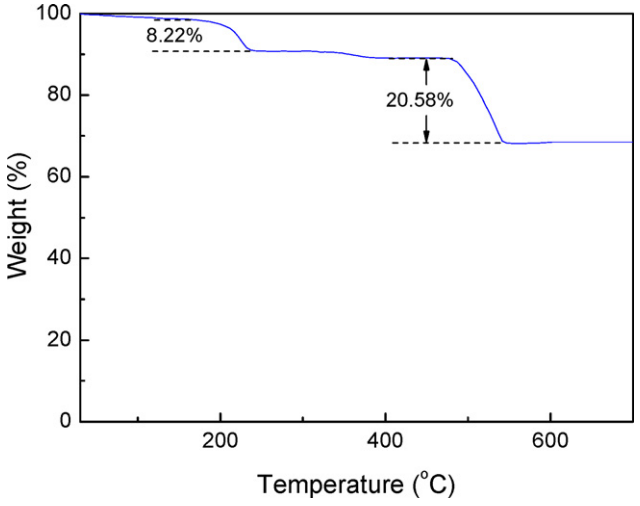

Fig. 5. TG profile generated by heating the mixture of cobalt hydroxide and potassium borohydride ($Co(OH)_2/KBH_4 = 1:2$).

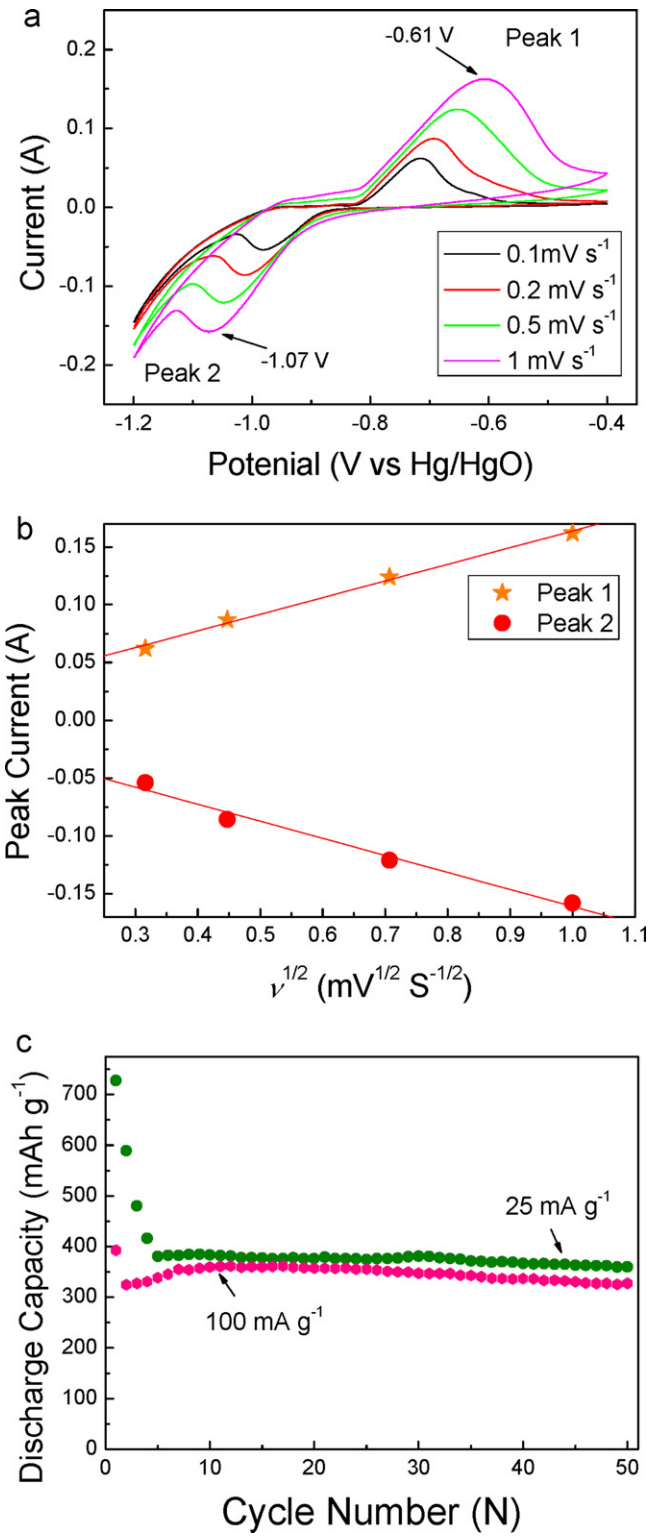

Fig. 6. Typical CV curves of orthorhombic CoB electrode at different scan rates (a) and the liner relationship between the peak current and the square root of the scanning rate $\nu^{1/2}$ (b). (c) Cycling performance of orthorhombic CoB electrode at different current rates.

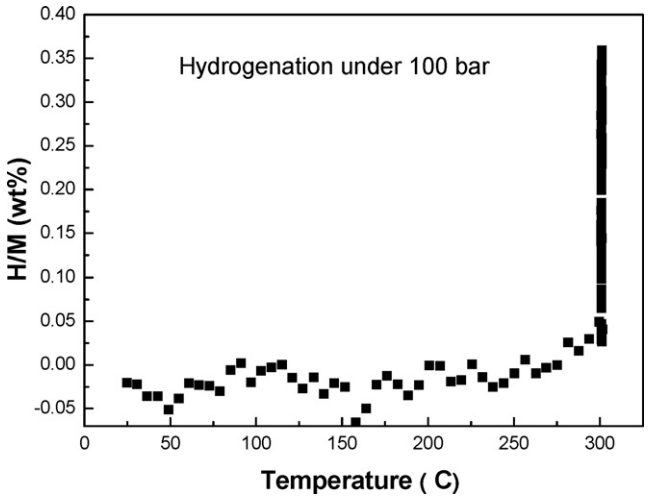

Fig. 7. Hydrogen absorption curves (H/M–T) for orthorhombic CoB sample.

This crystalline CoB electrode shows better electrochemical activity than previously reported [13–18].

3.4. Electrode reaction mechanism

There are two possible reaction mechanisms for the anode material of nickel-based secondary batteries, electrochemical hydrogen absorption–desorption mechanism and oxidation–reduction mechanism. For the former, the anode material must have the hydrogen storage properties. Thus, the hydrogen absorption properties of orthorhombic CoB are studied and illustrated in Fig. 7. There is no obvious hydrogen absorption for CoB even in high temperature and hydrogen pressure. Therefore, we conclude that CoB is not a hydrogen storage material, and its electrochemical capacity should not be attributed to the electrochemical hydrogen desorption.

To further investigate the reaction mechanism of CoB electrode, the XRD patterns at different cycles are acquired and reported in Fig. 8. At the 1st charge, there is no obvious change for CoB electrode. However, some diffraction peaks of $Co(OH)_2$ appear in the 1st discharged electrode. This indicates that the electrode is transformed from CoB to $Co(OH)_2$ during the 1st cycle. After the 2nd cycle, the diffraction peaks of CoB disappear, while the peaks of $Co(OH)_2$ become stronger, further confirms the conversion of CoB to $Co(OH)_2$. At the 10th charge, some diffraction peaks of Co are detected while those of $Co(OH)_2$ still exist. However, the diffraction peaks of $Co(OH)_2$ become stronger and those of Co become weaker in the 10th discharged electrode, illustrating that some Co are transformed into $Co(OH)_2$ during the discharge.

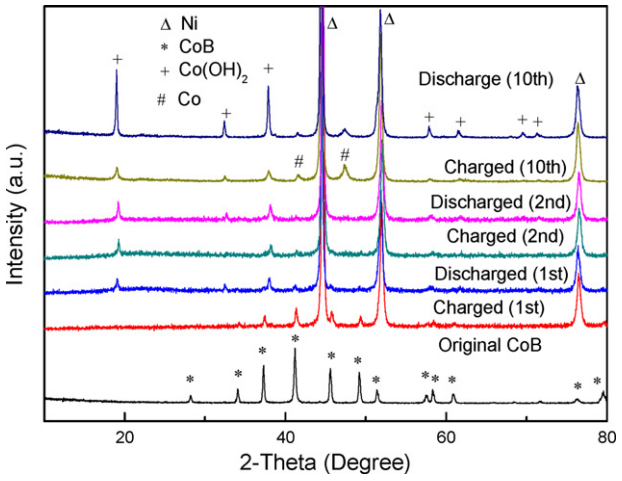

Fig. 8. XRD patterns of CoB electrode at different cycles.

Based on these experimental facts, we conclude a possible reaction mechanism of CoB electrode. CoB alloy is composed by Co and B in 0 oxidation. At the initial several cycles, Co is gradually oxidized into $Co(OH)_2$, while B is gradually dissolved in 6 M KOH [18]. Then, Co and $Co(OH)_2$ are mutually transformed during the charge–discharge process. The charge–discharge reaction can be expressed as follows:

$$Co + 2OH^- \underset{\text{charge}}{\overset{\text{discharge}}{\rightleftarrows}} Co(OH)_2 + 2e \quad (2)$$

The reversible electrochemical capacity of CoB electrode is attributed to the electrochemical oxidation of Co to $Co(OH)_2$. It is worthwhile to point out that B in CoB will provide some holes in the electrode when they are dissolved in KOH, which is useful to increase contact area of the electrode to KOH and improve its electrochemical performance. This is similar to the function of amorphous S on $Co(OH)_2$ electrode reported [25], which is the reason that the discharge capacity of CoB is higher than that of Co. Moreover, it could be concluded that the theoretical capacity of CoB is higher than other Co compounds because B is the lightest non-metallic element.

4. Conclusion

In summary, pure and high thermal stable orthorhombic CoB has been successfully prepared *via* the solid phase reaction between cobalt hydroxide and potassium borohydride, and electrochemically used as anode material for nickel-based secondary batteries. The reversible discharge capacities of the orthorhombic CoB electrode obtained are about 380 mAh g^{-1} at a discharge current of 25 mA g^{-1} and 360 mAh g^{-1} at 100 mA g^{-1}, exhibiting excellent cycling performance and rate capability. The reversible electrochemical capacity of CoB electrode is attributed to the electrochemical oxidation of Co to $Co(OH)_2$. To the best of our knowledge, the synthesis of orthorhombic CoB employing such a solid phase reaction is reported for the first time, and it shall be possible to extend this method for preparing other transition metal borides such as TiB_2, FeB, and NiB. Further studies are underway to broaden the applicability of this method.

Acknowledgements

This work was financially supported by MOST project (2010CB631303), NSFC (50701025 and 50971071) and MOE (IRT-0927).

References

[1] J. Van Wonterghem, S. Morup, C.J.W. Koch, S.W. Charles, S. Wells, Nature 322 (1986) 622.
[2] W.L. Johnson, Prog. Mater. Sci. 30 (1986) 81.
[3] Á. Molnár, G.V. Smith, M. Bartók, Adv. Catal. 36 (1989) 329.
[4] Y. Chen, Catal. Today 44 (1998) 3.
[5] J.F. Deng, H.X. Li, W.J. Wang, Catal. Today 51 (1999) 113.
[6] B. Ganem, J.O. Osby, Chem. Rev. 86 (1986) 763.
[7] S.E. Skrabalak, K.S. Suslik, Chem. Mater. 18 (2006) 3103.
[8] G.N. Glavee, K.J. Klabunde, C.M. Sorensen, G.C. Hadjipanayis, Inorg. Chem. 34 (1995) 28.
[9] C.A. Brown, V.K. Ahuja, J. Org. Chem. 38 (1973) 2226.
[10] Y. Zhu, F.P. Liu, W.P. Ding, X.F. Guo, Y. Chen, Angew. Chem. Int. Ed. 45 (2006) 7211.
[11] H. Li, C.Z. Wang, Q.F. Zhao, H.X. Li, Appl. Surf. Sci. 254 (2008) 7516.
[12] H. Li, H.X. Yang, H.X. Li, J. Catal. 251 (2007) 233.
[13] M. Mitov, A. Popov, I. Dragieva, J. Appl. Electrochem. 29 (1999) 59.
[14] Y.D. Wang, X.P. Ai, H.X. Yang, Chem. Mater. 16 (2004) 5194.

[15] Y.D. Wang, X.P. Ai, Y.L. Cao, H.X. Yang, Electrochem. Commun. 6 (2004) 780.
[16] D.G. Tong, W. Chu, X.L. Zeng, W. Tian, D. Wang, Mater. Lett. 63 (2009) 1555.
[17] D.S. Lu, W.S. Li, X. Jiang, C.L. Tan, R.H. Zeng, J. Alloys Compd. 485 (2009) 621.
[18] Y. Liu, Y.J. Wang, L.L. Xiao, D.W. Song, Y.P. Wang, L.F. Jiao, H.T. Yuan, Electrochim. Acta 53 (2008) 2265.
[19] J.Y. Shen, Z.Y. Li, Q.J. Yan, Y. Chen, J. Phys. Chem. 97 (1993) 8504.
[20] M.I.S.T. Faria, T. Leonardi, G.C. Coelho, C.A. Nunes, R.R. Avillez, Mater. Charact. 58 (2007) 358.
[21] Y. Liu, Y.J. Wang, L.L.D. Xiao, W. Song, L.F. Jiao, H.T. Yuan, Electrochem. Commun. 9 (2007) 925.
[22] Y. Bai, C. Wu, F. Wu, L.X. Yang, B.R. Wu, Electrochem. Commun. 11 (2009) 145.
[23] F. Izumi, I. Ikeda, Mater. Sci. Forum 321–324 (2000) 198.
[24] A.G. Ostroff, R.T. Sanderson, J. Inorg. Nucl. Chem. 4 (1957) 230.
[25] D.W. Song, Y.J. Wang, Q.H. Wang, Y.P. Wang, L.F. Jiao, H.T. Yuan, J. Power Sources 195 (2010) 7115.